1-1-2014

Optimal design of semi active control for adjacent buildings connected by mr damper based on integrated fuzzy logic and multi-objective genetic algorithm

Mehmet Uz
University of Wollongong, meuz@uow.edu.au

Muhammad N. S Hadi
University of Wollongong, mhadi@uow.edu.au

Optimal design of semi active control for adjacent buildings connected by mr damper based on integrated fuzzy logic and multi-objective genetic algorithm

Abstract

An optimal design strategy based on genetic algorithms (GA) is proposed for nonlinear hysteretic control devices that prevent pounding damage and achieve the best results in seismic response mitigation of two adjacent structures. An integrated fuzzy controller is used in order to provide the interactive relationships between damper forces and input voltages for MR dampers based on the modified Bouc-Wen model. Furthermore, Linear Quadratic Regulator (LQR) and H2/LQG (Linear Quadratic Gaussian) controllers based on clipped voltage law (CVL) are also used to compare the results obtained by fuzzy controller. This study employs the main objectives of the optimal design that are not only to reduce the seismic responses but also to minimize the total cost of the damper system. A set of Pareto optimal solutions is also conducted with the corresponding results obtained from the optimal surface of Pareto solutions in this study. As a result, decreasing the number of dampers does necessarily increase the efficiency of the system. In fact, reducing the number of dampers for the dynamic response of the system can contribute more than increasing the number of dampers.

Keywords

design, semi, active, control, adjacent, buildings, connected, mr, damper, integrated, fuzzy, logic, multi, objective, optimal, genetic, algorithm

Disciplines

Engineering | Science and Technology Studies

Publication Details

Uz, M. & Hadi, M. N. S. (2014). Optimal design of semi active control for adjacent buildings connected by mr damper based on integrated fuzzy logic and multi-objective genetic algorithm. Engineering Structures, 69 (June), 135-148.

elsevier_JEST_4859

Optimal ~~Design~~ design of ~~Semi~~ semi ~~Active~~ active ~~Control~~ control for ~~Adjacent~~ adjacent ~~Buildings~~ buildings ~~Connected~~ connected by MR ~~Damper~~ damper ~~Based~~ based on ~~Integrated~~ integrated ~~Fuzzy~~ fuzzy ~~Logic~~ logic and ~~Multi~~multi-~~Objective~~ objective ~~Genetic~~ genetic ~~Algorithm~~algorithm

Mehmet E. Uz

Muhammad N.S. Hadi*

mhadi@uow.edu.au

School of Civil, Mining & Environmental Engineering, University of Wollongong, Wollongong, NSW 2522, Australia

*Corresponding author.

Abstract

An optimal design strategy based on genetic algorithms (GA) is proposed for nonlinear hysteretic control devices that prevent pounding damage and achieve the best results in seismic response mitigation of two adjacent structures. An integrated fuzzy controller is used in order to provide the interactive relationships between damper forces and input voltages for MR dampers based on the modified Bouc-Wen model. Furthermore, Linear Quadratic Regulator (LQR) and H_2/LQG (Linear Quadratic Gaussian) controllers based on clipped voltage law (CVL) are also used to compare the results obtained by fuzzy controller. This study employs the main objectives of the optimal design that are not only to reduce the seismic responses but also to minimize the total cost of the damper system. A set of Pareto optimal solutions is also conducted with the corresponding results obtained from the optimal surface of Pareto solutions in this study. As a result, decreasing the number of dampers does necessarily increase the efficiency of the system. In fact, reducing the number of dampers for the dynamic response of the system can contribute more than increasing the number of dampers.

Keywords: Adjacent ~~Buildings~~buildings; Semi-active control; Clipped-optimal algorithm; Magneto-~~Rheological~~ rheological (MR) damper

1 Introduction

In structural design it is necessary that the total displacement and the inter-storey drift of the structures should be limited whereas the absolute acceleration must be kept small for the human comfort. Structures with installed fluid visco-elastic dampers (VEDs) [1–4], friction dampers [1–5], active devices [6–9] and semi-active magnetorheological (MR) dampers [10–13] systems have been introduced for the human comfort in today's modern concepts. The control systems that are optimized using the procedures developed in previous studies [14–16] are capable of mitigating the response of the structure. Several types of dampers have been studied onto structures as paramount interest over the past two decades. Despite high-rise buildings being constructed in close proximity, various methodologies of interconnecting adjacent buildings have been examined for seismic hazard mitigation. Despite the development of recent control strategies like semi-active control, research in the area of passive and active structural control is still continuing [17].

According to stochastic response of the building in the parametric study of Kim et al. [18], there is a certain size of fluid visco-elastic dampers to minimize the response of the structures subject to white noise and earthquake excitation. In recent years, owing to the adaptability of semi-active control devices, considerable attention has been directed to research and development. One such innovative device is the magnetorheological (MR) damper, which utilizes MR fluids for providing control capability. A MR damper offers a highly reliable mechanism for response reduction at a modest cost, and is fail-safe because the damper becomes passive if the control hardware breaks down [19]. Dyke et al. [20], Ni et al. [21], Park and Ok [22] and Kim and Kang [23] have investigated the effectiveness of MR dampers for civil engineering structures. A wide range of theoretical and experimental studies of a 20-tonne MR damper at the University of Notre Dame have demonstrated that MR devices can provide forces of the magnitude required for full-scale structural control applications [24].

For the optimization of damper parameters, Luco and De Barros [25] investigated the optimal damping values for the distribution of passive dampers. In general, analytical and experimental studies have investigated the dynamic responses of the structures before and after installing a damping device to understand their effectiveness. However, very little study has been done with regard to the effect of non-uniform distribution of the dampers [3,6,14,15]. None of these studies show a clear comparison so as to signify the quality of their own proposed arrangement/solution. For example, Bhaskararao and Jangid [6] proposed a parametric study to investigate the optimum slip force of the dampers in the responses of two adjacent structures. The authors also confirmed that the response reduction is associated with optimum placement of dampers. Yang et al. [3] showed that in order to minimize loss in performance the number of dampers can be decreased. The authors showed that it is not necessary to equip every single floor with a viscous damper in accordance with the solution of trial and error. But no solution for the optimal arrangement was provided.

A similar study for MR dampers conducted by Bharti et al. [15] proposed that the placement of damper is not ~~neccessary~~necessary for every single floor. Bharti et al. [15] also confirmed the results obtained by Ok et al. [14] which studied the ~~performence~~performance of adjacent buildings equipped with MR dampers by the use of genetic algorithms. As an attempt to bring a clear method to provide the optimal arrangement, Bigdeli et al. [26] introduced optimization algorithms to find the optimal configuration for a given number of dampers. For the purposes of ~~comprasion~~comparison, the authors also used the highest relative velocity heuristic approach based on the work of Uz [27]. Uz and Hadi [28,29] proposed that fluid viscous dampers should be placed in floors where the maximum relative velocity occurs. This work was ~~repated~~repeated by Patel and Jangid [30].

For developing other recent control strategies, various control algorithms developed for passive, semi-active and active control have been directly useful. The most common optimal control algorithms such as Linear Quadratic Regulator (LQR), H_2/LQG (Linear Quadratic Gaussian), H_2, H_∞ and the FLC theory can be chosen with combining the GAs. The fuzzy logic control (FLC) theory has attracted the attention of engineers during the last few years [16,31], there are some drawbacks in FLC systems. The fuzzy sets and rules that require a full understanding of the system dynamics must be correctly pre-determined for the system to function properly. Furthermore, in order to mitigate the responses of a seismically subjected civil engineering structures, multiple MR dampers distributed between the adjacent buildings should be used [16]. Zhou et al. [32] successfully applied an adaptive fuzzy control strategy for control of linear and nonlinear structures. The authors found that the adaptive feature of a fuzzy controller has various advantages in the control of a building including a MR damper system.

Another trend in the development of a FLC system is to combine genetic algorithms (GA) as an optimization tool in designing control systems [26,33–39]. Optimizing the dampers to mitigate seismic damage for adjacent buildings has hitherto not been investigated well in spite of enhancing structural control concepts in the structural vibration control through the application of optimization in an integrated genetic algorithm (GA)–FLC. Based on the improvements in the fuzzy logic controller for multiple mode contributions, nonlinear base isolated structures using semi active devices together with passive devices in a hybrid manner were investigated in order to utilize a set of bench mark problems [40,41]. Ahlawat and Ramaswamy [42] proposed an optimum design of dampers using a multi-objective version of the GA. Arfiadi and Hadi [36] improved a simple optimization procedure with the help of GAs to design the control force. They used a static output feedback controller utilizing the measurement output. For obtaining the best results in the reduction of the structures, combined application of the GAs and FLC has been proposed to design and optimize the different parameters of active dampers by Pourzeynali et al. [43].

In this study, the optimal design of semi-active dampers placed between adjacent buildings is investigated into two different sections. In the first section, an adaptive method for the design of a FLC system for protecting adjacent buildings under dynamic hazards using MR dampers is proposed by using single GA. The design of the genetic adaptive fuzzy (GAF) controller is described in the first section of this study. Minimizations of the peak inter-storey drift and displacement related to ground responses are the two objectives of this study. A global optimization method which is a modification of the binary coded genetic algorithm adopted by Arfiadi and Hadi [35,36] has been used. Binary coded GA is used to derive an adaptive method for selection of fuzzy rules of the FLC system. The fuzzy correlation between the inputs (structural responses) and the outputs (command voltages) of the controller is provided with adding, changing and deleting the rules of the FLC system. Inputs are taken as the top floor displacements of both buildings. Nevertheless, the binary coded GA automatically employs and optimizes the fuzzy controller in accordance with the fitness function that reflects the multiple objectives. The last section presents results of this study which show that not only there is a reduction of seismic responses of the adjacent buildings but also the total cost of the damper system is reduced. Therefore, the peak inter-storey drift response and the total number of nonlinear dampers constitute the objective functions of the optimization problem for two buildings.

This study uses two groups of design variables of the optimization. The first group of variables relate to whether a damper exists or not between each of the floors of the buildings. Cleary these floors relate to the shorter building. In order to achieve the objectives of this study, dampers are proposed to be installed between the two buildings of each floor up to the top floor of the shorter building. The existence of these dampers and their corresponding voltages are design variables of this study. The design process uses the excitations of the NS components of the El-Centro 1940 and Kobe 1995 ground acceleration records. Numerical results of adjacent buildings controlled with MR dampers and the corresponding uncontrolled result are examined and compared with nonlinear control algorithms.

2 System description

Two n and m storey shear buildings with semi-active dampers installed between them as shown in Fig. 1 are considered. With combining integrated fuzzy logic and GA, the top floor displacements of the adjacent buildings are used as the inputs of a fuzzy controller. The fuzzy controller outputs command voltages in order to control MR dampers for generating damping force.

$$\Lambda = \begin{bmatrix} P_1 \\ 0 \\ P_2 \end{bmatrix},\ \Gamma = \begin{bmatrix} -M_1 E_1 \\ -M_2 E_2 \end{bmatrix},\ A = \begin{bmatrix} 0_{(n+m)\times(n+m)} & \mathbf{I}_{(n+m)\times(n+m)} \\ -M^{-1}K & -M^{-1}C \end{bmatrix} \quad (1)$$

$$E = \begin{bmatrix} 0_{(n+m)\times 1} \\ M^{-1}\Gamma \end{bmatrix},\ B = \begin{bmatrix} 0_{(n+m)\times n_a} \\ M^{-1}\Lambda \end{bmatrix}$$

where E_1 and E_2 are $n \times 1$ and $m \times 1$ unity matrices, respectively. P_1 and P_2 are given as $m \times n_a$ matrices based on the number of actuators of the additional dampers (n_a). m denotes the storey number of the lower building. Here, **I** is an

identity matrix and 0 in Λ matrix is a $(s \times n_a)$ matrix containing zero. $F_{mr} = \begin{bmatrix} f_{mr}^1 & \cdots & f_{mr}^i f_{mr}^m \end{bmatrix}^T$ is control input vector. The equation of motion in Eq. (1) can be arranged as

$$\dot{X} = AX + BF_{mr}(t) + E\ddot{X}_g(t) \tag{2}$$

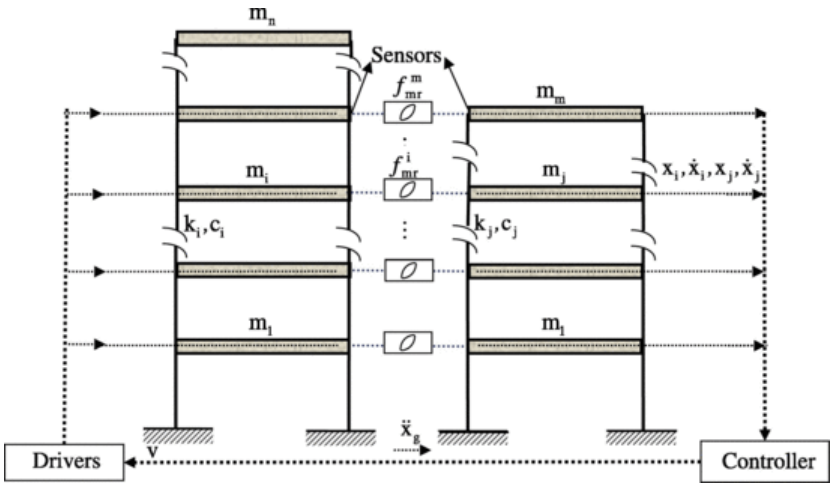

Fig. 1 *N* and *M* storey shear buildings with MR dampers.

As mentioned above, the control objective in single objective GA is to minimize both the peak displacement and inter-storey drift responses of the adjacent buildings to provide safety of both buildings and maintain an acceptable level of comfort for the occupants.

2.1 MR damper forces

For the first time, Spencer Jr et al. [44] presented the MR dampers force through applying the Bouc-Wen model. The modified Bouc-Wen model was used to simulate the dynamic behavior of the MR damper that involves voltage-dependent parameters to model the fluctuating magnetic fields [44]. The applied force of this model is given by

$$f_{mr}^i = c_1\dot{y}_i + k_1(x_{i+n} - x_i - x_0) \tag{3}$$

where the internal pseudo-displacement, $\dot{y}_i$ and the evolutionary variable, $\dot{z}_{di}$ are given by

$$\dot{y}_i = \frac{1}{(c_0 + c_1)}\{\alpha z_{di} + c_0(\dot{x}_{n+i} - \dot{x}_i) + k_0(x_{n+i} - x_i - y_i)\}$$

$$\dot{z}_{di} = -\gamma|\dot{x}_{n+i} - \dot{x}_i - \dot{y}_i|z_{di}|z_{di}|^{n_d-1} - \beta(\dot{x}_{n+i} - \dot{x}_i - \dot{y}_i)|z_{di}|^{n_d} + A_c(\dot{x}_{n+i} - \dot{x}_i - \dot{y}_i) \tag{4}$$

where x_i and x_{n+i} are the displacements of the ith floor of Building A and Building B, respectively. The displacement of the MR damper Δx_i is computed using the relative displacement between two inline adjacent floors (i). x_0 is the initial displacement of spring of the accumulator stiffness k_1. k_0 is the stiffness at large velocities. c_0 and c_1 are viscous damping at large velocities and nonlinear roll-off in the force–velocity loops at low velocities, respectively. α is the evolutionary coefficient. Other shape parameters of the hysteresis loop are shown as γ, A_c, n_d and β in Eq. (4). In this model, Spencer Jr et al. [44] have suggested for the dependence of the force on the voltage applied to the current driver and the resulting magnetic current as

$$\alpha = \alpha_a + \alpha_b u; \quad c_1 = c_{1a} + c_{1b}u; \quad c_0 = c_{0a} + c_{0b}u \tag{5}$$

Here, u is given as the output of a first-order filter which models delay dynamics of the current driver and of the fluid to reach rheological equilibrium. Eq. (6) is necessary to simulate the dynamics involved in both reaching rheological equilibrium and driving the electromagnet in the MR damper. The dynamics are accounted for through the first order filter

$$\dot{u} = -\eta(u - v_i) \tag{6}$$

where v_i is a command input voltage supplied to the damper at *i*th floor. f_{mr}^{i} is the damper force at the *i*th floor level between the buildings. Parameter variables that were obtained by Spencer Jr et al. [44] by optimal fitting their model to test data are given in Table 1 and used in this study.

Table 1 Parameters of Bouc-Wen phenomenological model parameters for 1000 kN MR dampers.

Parameter	Value	Parameter	Value
c_{0a}	50.30 kN sec/m	α_a	8.70 kN/m
c_{0b}	48.70 kN sec/m/V	α_b	6.40 kN/m/V
k_0	0.0054 kN/m	γ	496.0 m^{-2}
c_{1a}	8106.2 kN sec/m	β	496.0 m^{-2}
c_{1b}	7807.9 kN sec/m/V	A_c	810.50
k_1	0.0087 kN/m	n_d	2
x_0	0.18 m	η	195 sec^{-1}

2.2 Clipped optimal control design

The input voltage, *v*, to the damper is obtained using the clipped voltage law (CVL) [20] as described below. If these two forces are equal then the applied voltage is not changed. If the absolute of MR damper force is less than the absolute of the calculated optimal control force and both of them have the same sign, the applied voltage should be increased to its maximum value. Otherwise, the input voltage is set to zero. Clipped-optimal method can be summarized in the following equation.

$$v = V_{max}\mathbf{H}\{(f_d - F_{mr})F_{mr}\} \tag{7}$$

where V_{max} is the maximum applied voltage that is associated with the saturation of the magnetic field in the MR damper and **H**{·} is the Heaviside function. The voltage applied to the MR damper should be V_{max} when **H**{·} is greater than zero. Otherwise, the command voltage is set to zero.

The main limitation stems from using semi active devices appear for the clipped optimal strategy. The strategy tries to change the voltage of the MR damper from zero to its maximum value, which makes the control force sub-optimal. Moreover, sometimes this swift change in voltage and therefore sudden rise in external control force increases the system responses, which may lead to an inelastic response of the structure. Therefore there was a need for better control algorithms that can change the MR damper voltage slowly and smoothly, such that all voltages between maximum and zero voltage can be covered based on the feedback from the structure using the proposed method by GA.

3 Optimum design of damper system

The main goal of using dampers is to reduce the inter-storey drift, which is denoted as the relative displacement between two successive floors in the study. This study has another aim which is to minimize the total number of MR dampers for economical benefits. Thus, the design of a damper system can be optimally possible using a multi objective optimization formulated as

$$Minimize\begin{bmatrix} \max\limits_{i=1,2...,n+m}\{\Delta d_i\} \\ ndi \end{bmatrix} \tag{8}$$

where Δd_i is the root-mean-square (r.m.s.) inter-storey drift of the *i*th floor of the coupled structural system and *ndi* is the total number of installed dampers. Combining multiple objective functions into a single-objective function by use of arbitrary importance weights are often done in a conventional optimization approach [45]. However, prior knowledge of the relative importance of multiple objective functions is not practically feasible for an optimization problem. In other words, in a single objective function it is not easy to decide on weighting factors which show the relative importance of two different physical quantities such as the number of dampers and the maximum drift responses. Therefore, this study implements a multi objective optimization approach to obtain a method of optimal designs known as Pareto-optimal solutions and adopts a procedure to choose a reasonable design. Details of an optimization problem for minimizing two objective functions are given in the study of Ok et al. [45,46]. Any of the objective functions can be considered as an acceptable solution as long as none of the solutions on the optimal surface is absolutely better than any other. Pareto-optimal or non-dominated solution set denotes as a set of optimal solutions in this study.

Goldberg [47] suggested a non-dominated sorting procedure in conjunction with a sharing technique. Consequently, for the multi-objective optimization of nonlinear dampers, Srinivas and Deb [48] presented a non-dominated sorting genetic algorithm (NSGA) which follows the conventional single-objective genetic algorithm (SOGA) except for the ''elitist'' and ''fitness assignment'' operations. In this study, firstly, the binary coded SOGA is described below.

3.1 Binary coded the SOGA

GA is an effective tool for solving optimization problems in engineering applications. Binary string in GA can represent a candidate of a design variable. GA used binary coding to represent the design variable at its early development [47,49]. After initializing, the fitness of candidates is calculated according to the objective function. The genetic algorithm process is shown in Table 2. The candidates undergo selection process based on the fitness of each individual. In the selection process, the better chromosomes generate higher values than others and place it in the mating pool. Every individual (chromosome) of the design variables (genes) in the population undergoes genetic evolution through crossover and mutation by a defined fitness function. In this study, the roulette wheel selection procedure maps the population in conjunction with the elitist strategy. By using elitist strategy, the best individual in each generation is ensured to be passed to the next generation. After selection, crossover and mutation, a new population is generated in both GA codings. This new population repeats the same process iteratively until a defined condition. Details of the genetic algorithm structures are given below. In this study, binary coding is used for adjacent buildings connected by semi-active dampers. Briefly, the binary coding is presented below.

Table 2 Structure of genetic algorithm.

Start (1)
Generation: $\tau \leftarrow 0$ % τ is iteration number
Initialize $G(\tau)$ % $G(\tau)$: Population for iteration
Evaluate $f(G(\tau))$ % $f(G(\tau))$: Fitness Function
while (not termination condition) do
start (2)
$\tau \leftarrow \tau + 1$
Perform operation of selection
Determine the number of crossover based on p_c
Select the two parents $\widetilde{G}, \overline{G}$ from $G(\tau - 1)$
Perform crossover operation
Perform mutation operation for the whole population based on p_m
Insert a number of new random individuals replacing old individuals
Evaluate $f(G(\tau))$
end (2)
end (1)

3.2 Design variables

In the binary coding GA, by using a binary string having 1 or 0, the chromosome can be shown. The mechanics of GA starts with creating an initial population of chromosomes as a set of candidates of initial design variables. The length of sub-chromosome (*nbits*) can be calculated based on upper (U_i) and lower (L_i) bound values and the significant digit (P_i) of each design variable (i). It is clear that the length of sub-chromosome depends on the required precision (P_i) of the design variable. Details of the length of the individual is described by Arfiadi [33]. On the other hand, in real coding, as the candidates of design variables, real coding GA uses vectors of real numbers to represent individuals. After converting binary chromosome into real values of design, the population of the individuals can be shown as follows

$$\text{Population} \begin{vmatrix} 1^{\text{st}} \text{ chromosome} \\ I^{\text{th}} \text{ chromosome} \\ \vdots \\ P^{th} \text{ chromosome} \end{vmatrix} \begin{matrix} G^1 = [g_1^1 \quad g_2^1 \quad . \quad . \quad g_r^1] \\ G^2 = [g_1^2 \quad g_2^2 \quad . \quad . \quad g_r^2] \\ \vdots \\ \vdots \\ G^p = [g_1^p \quad g_2^p \quad . \quad . \quad g_r^p] \end{matrix} \tag{9}$$

where g_j^i represents an element of the ith individual of the jth design variable. For example, $r = (n_a \times m_a)$ controller gains having the both n_a actuators to drive the control force and m_a measurements are to be obtained for the feedback.

3.3 Procedure of GA

In binary coding, after initialization, the conversion of binary strings into a real number of design variable is performed using Eq. (10) [39].

$$r_i = L_i + \frac{t_i \times (U_i - L_i)}{2^{nbits} - 1} \tag{10}$$

where r_i is the real number of a design variable. t_i is an integer mapping of a binary string which can be obtained using

$$t_i = \sum_{j=0}^{l_m} h_j \times 2^j \tag{11}$$

In which the binary bit h_j is as follows $[h_r \quad h_{r-1} \quad \dots \quad h_1 \quad h_0]$ and l_m is the length of sub-chromosome to represent a particular design variable –1. The fitness of each individual can be obtained according to the defined objective function after determining the real value of each design variable in the population. This function reflects the desired objective. The control objective is to minimize both the peak displacement and peak drift responses of the structure to ensure the safety of the building and maintain the comfort level of the occupants. A set of evaluation criteria based on those used in the second generation linear control problem for buildings to evaluate the various control algorithms are given [50,51]. In this study, three of those criteria which are also regarded as the objectives in GA are selected to evaluate the effectiveness of the proposed method. The first evaluation criterion is a measure of the normalized maximum floor displacement relative to the ground and the peak drift given as

$$J_1 = \max_{t,i}\left(\frac{|x_i(t)|}{x^{\max}}\right) \quad \text{or} \max_{t,i}\left(\frac{|d_i(t)|}{d^{\max}}\right) \tag{12}$$

where $x_i(t)$ is the relative displacement of the ith floor over the entire response, and x^{max} denotes the uncontrolled maximum displacement response. $d_i(t)$ is the inter-storey drift of the ith floor $(x_i - x_{i-1})$, which is normalized by the peak uncontrolled floor drift denoted as d^{max}. The other evaluation criterion is the total number of MR dampers installed at floors given by

$$J_2 = N_d \tag{13}$$

The evaluation criterion, J_3, is the resulting γ in the H_∞ norm to be determined for the parameters of damper c_d, k_d because of installation of MR dampers. For simplicity, the objective function that reflects the above objectives in this study is defined as follows

$$J = \alpha_c J_1 + \frac{(1 - \alpha_c)}{2}(J_2 + J_3) \tag{14}$$

where J_1, J_2 and J_3 are the evaluation criteria defined above representing normalized maximum floor displacement relative to the ground or normalized peak floor drifts, total number of dampers and damper parameters respectively. α_c is a weighting coefficient reflecting the relative importance of the three objectives. Each individual into the fitness function calculates the fitness of each individual. The positive fitness function is needed in GA, the problem of minimization is converted such that the fitness has a positive value. Then the objective value is converted to fitness value given by

$$F = (C_p - J) \times \mu \tag{15}$$

where C_p is a proper constant to make sure the fitness value is positive. μ is a penalty constant to scale the fitness function. Semi-active control system may cause instability if not designed properly. To avoid the instability of the structure, the simplest way is to ensure that the eigen-values of the closed loop system are placed in the left side of the s-plane. This constraint is incorporated to the fitness function by simply setting the fitness of the individuals having positive real-part eigen-value to a very small positive value that can still be accepted by the computer. If the system has a negative real part of the eigen-value then the system is called asymptotically stable [52]. This fitness function forms the basis of the genetic operations in this study.

The selection procedure used in this study is a roulette-wheel selection procedure in binary coding. The reproduction is processed in two stages. In the first stage, the fitness of each individual is evaluated and the sum of the fitness is calculated in order to determine the probability of selecting each chromosome. In the second stage, the selection mechanism picks the highly fitted chromosomes into the mating pool. To perform this stage, the cumulative probabilities of selecting each individual are calculated [36,38,39]. Each random number a_j ($j = 1, 2, \dots$ popsize) between 0 and 1 is compared with the cumulative probability of selecting each chromosome q_j and when the random number $a_j \leqslant q_j$, the jth individual will be selected. Here, popsize is the number of the individual in the population. The best individual is always selected in the next generation using an elitist strategy by simply passing the best fitness individual into the next generation. After selection has been carried out, the crossover and mutation operations are performed.

In this study, a simple crossover is used as the main crossover operator for binary coding. Simple crossover randomly picks two parents from the mating pool. Simple crossover exchanges genetic information for one random split point in the

chromosomes. Two chromosomes are chosen for a simple crossover operation if the random number is smaller than the crossover rate p_c. Details of a simple crossover operation can be referred to Holland [49] and Michalewicz [52]. After a simple crossover in the binary coding, mutation is performed. Mutation is a random operator whereby values of element within a chromosome are modified. $p_m \times (ntbits \times popsize)$ bits will undergo for mutation operator if a random number n_r from the range (0–1) < p_m. Here, *ntbits* is sum of the length of chromosomes (*nbits*). In this case, the mutation is run with the probability of mutation p_m. In order to maintain the variability of the population, mutation in binary coding is the random changing of 0–1s and vice versa.

3.4 NSGA approach

The NSGA approach [48,53] requires the ''rank-based sorting'' after the fitness assignment progress. It ranks the non-domination of the individuals in the population based on the vectors of multiple objective functions. At this stage, the rank and the crowding distance for each chromosome is added to the chromosome vector for ease of computation [48,53]. Then, the set of solutions corresponding to the most non-dominated set is saved during the elitist operation. In the following set, a ''niche-based sharing'' procedure is performed to provide a diverse search direction along the Pareto-optimal surface by degrading the fitness of densely populated individuals. Based on the fitness values, the next generation of the population is produced through the selection, crossover and mutation operations.

4 Design of fuzzy controller in GA

Since the correlation between the structural responses and the command voltages is difficult to determine in a conventional design approach, especially for a MIMO system, GA is introduced as an effective method to optimally design the fuzzy controller. In an ordinary design approach, the membership functions and control rules of a fuzzy controller are usually determined by trial and error which is a tedious and time consuming task. For efficiency, an optimal design of fuzzy control rules and membership functions of the fuzzy controller is desired. In this study, for simplicity, GA is only employed as an adaptive method for selection of fuzzy rules of the FLC system, and other parameters of the fuzzy controller such as the shape and the distribution of the membership functions are unchanged once defined. First, the input and output space of the system to be controlled is divided into fuzzy regions and the membership functions are defined as for design of an ordinary fuzzy controller. The integrated GA–FLC architecture uses GA to derive proper rules from the initial rules (however, the initial rules are not necessarily needed in this study).

4.1 Encoding the input–output region into bit-strings

Fig. 2 shows graphically the conceptual diagram of the proposed fuzzy control strategy. Encoding information is the most important step in the design of a controller. One of the biggest differences between GA and other optimization methods is that GA works in the genetic space; therefore, it is necessary to code the fuzzy input and output sets into genetic space represented by chromosomes. As can be seen in Fig. 2, the proposed fuzzy control strategy does not require a primary controller. The input voltage to the MR damper as input information from the response of the MR damper as output information can be obtained by the FLC. Composition of the fuzzy logic is four modules as fuzzification, rule-based, inference mechanism and defuzzification [54].

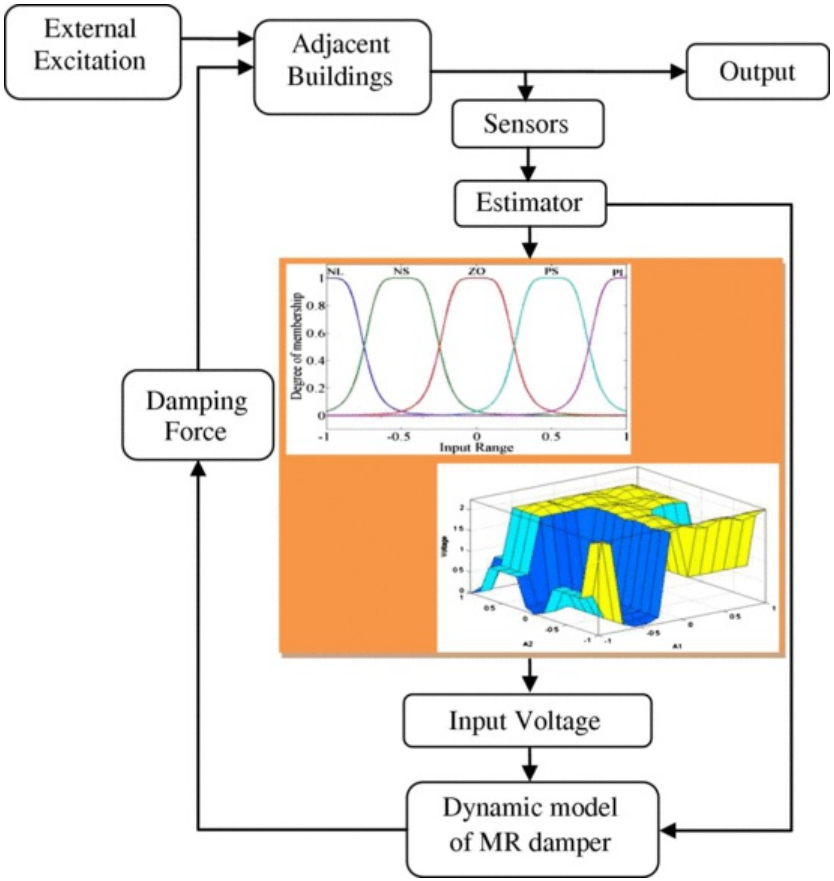

Fig. 2 Flowchart of semi-active fuzzy logic control system.

In order to be controlled into fuzzy regions and defining the membership functions, the design of the fuzzy controller begins with selection of a range of input values. Here, a fuzzy controller has been defined using a total of five membership functions for each of the inputs. A fuzzy set in this study is defined using five abbreviations as follows: NL (Negative Large), NS (Negative Small), ZO (Zero), PS (Positive Small) and PL (Positive Large). For the input membership functions, a reasonable range for each input value must be selected. For example, the outermost membership functions can be rarely utilized if the range is too large. Conversely, if the range is too small, the innermost membership functions are rarely utilized. Utilizing either the outermost or the innermost membership functions limits variability of the control system [16,31]. In order to avoid this limitation, 70–80% of the maximum uncontrolled displacement responses of the corresponding floors is taken as a reasonable range for each input in this study. The definition of the fuzzy output membership function abbreviations are as follows: ZO (Zero), S (Small), M (Medium) and L (Large) as shown in Fig. 3.

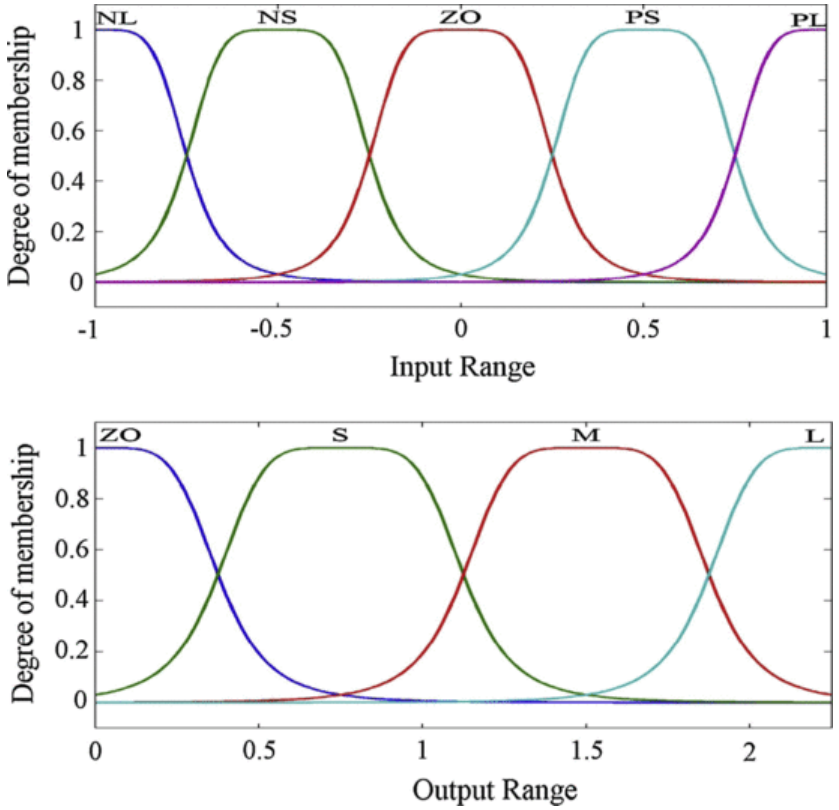

Fig. 3 Membership functions used for input and output variables.

The fuzzy output is the command voltage of MR damper and the range of output corresponds to the operational voltage range of the MR damper through an iteration process without a normalized voltage range. The command voltage indirectly determines the damping force of the MR damper. A generalized bell-shaped membership function is used in order to approximate almost all other types of membership functions. The shape of the generalized bell shape membership function can be defined by parameters. After all fuzzy rules are evaluated, the results of the rules are combined and defuzzified to a single number output. The expansion and contraction of the horizontal axis in the input membership function directly influence to define whether the output of the fuzzy logic is large or small. The rule-base module is constructed by specifying a set of if-and-then-consequent statements. A fuzzy logic control system with two inputs and single output represents each damper between adjacent buildings to be designed. This two-input–single-output case is chosen to simply clarify the basic ideas of how to represent a fuzzy rule base using bit-strings. Each input is divided into five fuzzy sets in this study. A fuzzy rule base consists of 25 fuzzy rules for the two fuzzy inputs. A five-by-five table with each cell to hold the corresponding outputs can be categorized for these rules. There are four choices for the voltage output corresponding to each rule.

For example, using ''IF-THEN'' form, IF Input 1 is ZO and Input 2 is PL, THEN Output 1 is M or L or ZO or S. The if-part of the rule is called the antecedent which involves fuzzifying the input and applying any necessary fuzzy operators, while the then-part of the rule is called the consequent known as implication. Each chromosome in the population consists of all the fuzzy rules and has the same input conditions but different output control signals assigned to bit-string. The bit-string is needed only to encode the output signals of the fuzzy rule. There are totally 25 rules that form the fuzzy control rule base, thus 100 bits in total can be used to represent a whole rule base for a single output. Each four consecutive bits are coded to represent the output for each rule. Each four bits from left to right represents the output linguistic variables ZO, S, M and L, respectively. An output signal is selected by GA by setting the corresponding bit to 1 while the other three bits are 0s [16]. For example, each 25 rule has four bits. Here, only 4 rules are given as an example. If Input 1 is NL and Input 2 is NL, then Output 1 is M. If Input 1 is NS and Input 2 is PS, then Output 1 is S. If Input 1 is ZO and Input 2 is ZO, then Output 1 is ZO. If Input 1 is PS and Input 2 is PL, then Output 1 is L. Thus, a chromosome can be represented as 100 bits in total.

The current voltage obtained from the FLC combined GA is the same for all dampers installed between the buildings. The proposed integrated fuzzy logic and GA control strategy is especially suitable for designing a MIMO system. The multiple damper cases are similar to the single damper case, except that the bit number that represents the corresponding output voltages has a longer length. For example, while the same current voltages used for n_j number of MR dampers at the j storey level, different current voltages can be used for different storey levels. If different current voltages are needed throughout 10 storey levels, 250 rules are determined by GA using 1000 bits chromosomes. However, the problem in this coding strategy is that it is hard to perform a mutation

operation since it may result in more than one choice for each output in one rule. So in this study, only the selection and crossover operators are used to perform GA operations while neglecting the mutation operator because crossover is the main evolution operator in GA and mutation is secondary.

Producing fuzzified outputs from the fuzzified inputs in the inference mechanism can be provided by means of the fuzzy rules in the rule base module. All fuzzy statements are resolved in the antecedent to a degree of membership between 0 and 2.25. After the entered and fuzzified input values, the fuzzy operator is applied to the antecedent and two fuzzified results are obtained as a single number. In this study, the *min* function for the *and* fuzzy operator (implication method) is used to determine the certainty of the fuzzy output variable for each fuzzy output. The truncated fuzzy set is defuzzified to assign single value to the output command voltage by using the max function. For defuzzification, the centroid calculation is used in this study as the most popular defuzzification method that is the last component of the fuzzy logic. This study adopts the centre of gravity (COG) method among defuzzification methods. The COG method is defined as follows:

$$y_i = \frac{\sum_{j=1}^{N_A} b_i^{(j)} \int \mu_{A_i}^{(j)}}{\sum_{j=1}^{N_A} \int \mu_{A_i}^{(j)}} \quad (16)$$

where N_A is the number of rules activated from the inputs, $\mu_{Ai}^{(j)}$ is the value of the output membership function in the consequent statement for the *j*th rule for *i*th input, $b_i^{(j)}$ is the centre of the output membership function $\mu_{Ai}^{(j)}$ and the integral of output membership function $\int \mu_{Ai}^{(j)}$ represents the area of the output membership function. By means of the rule base in the inference mechanism, FLC determines the control voltage to the MR damper using the input functions.

5 Solution procedure

A numerical example for adjacent buildings is performed on i7-2630QM @2.9 GHz computer running MATLAB R2011b. The GA built on the MATLAB numeric computing environment is integrated into the SIMULINK block to simulate the FLC controller. Furthermore, binary coding is used to optimize the semi-active device parameters with defining the regulated output to obtain the required voltage and number of dampers for each floor level.

The simple GA procedure is also slightly modified here. The GA parameters used in this study are separated into two sections as shown in Table 3. Some fresh individuals after selection, crossover and mutation are inserted into population and fresh individuals can help for exploring new candidates of the design points. Although some bad fitness individuals can pass into the next generation with inserting new individual, the average fitness of the current population will be better than the average of fitness of the previous population. As the optimum design, the best design points can be obtained in the final generation by copying the highest fitness value into the next generation.

Table 3 GA parameters used in this study.

GA parameters	Value
Number of generations	100
Population	12
Probability of crossover	0.8
Probability of mutation	0.01
Number of new random chromosomes to be inserted after crossover and mutation (%)	20

5.1 Numerical study

A system of buildings located adjacent to each other and interconnected by MR dampers is considered to obtain the optimal semi-active control strategies. Building A is a 20-storey shear building discussed in Bharti et al. [15] and Ok et al. [14]. A 10-storey building discussed in Kalasar et al. [55] and Pourzeynali et al. [43] is taken as Building B. The adjacent buildings are subjected to the 1940 El Centro (117 El-Centro Array -9 station) and the 1995 Kobe (KJMA station) excitations where the maximum ground acceleration scaled to 0.3 g for 1940 El Centro NS for long duration far field and 0.8 g for 1995 Kobe NS for pulse type near field, respectively. The structural parameters having mass, stiffness and damping coefficient are shown for both buildings in Table 4. A stiffness proportional damping is assumed in Building A with the damping ratio of the fundamental mode equals to about 5% while Building B has also 5% of damping ratio of the first mode. The first nine natural frequencies of the 20-storey building and the first five natural frequencies of the 10-storey building are given in Table 5. The effectiveness of the semi active device in each building for each earthquake signal given its frequency content and pulse nature is given in subsequent work of Hadi and Uz [56]. Fig. 4 shows the transfer function from external disturbance to the top floor of Building A. The effect of linking buildings with semi active control system compared with uncontrolled system can be observed from a peak magnitude in *bode* diagram. The designed adjacent buildings with damper provide the reduction of response of each building around the frequency of the first mode, where the highest contribution to response of each building is as shown in Fig. 4. For uniformity of the obtained results, GA was run four times as shown in Fig. 5. Similar optimal results were obtained from the four runs. The response is obtained with passive-off and passive-on cases which are with constant zero voltage and with constant maximum applied voltage of 10 V, respectively and compared with semi active control case. In this numerical example, the input voltage are taken as the range of 0–2.25 V for fuzzy logic controller. Hence, a maximum value of 2.25 V is shown in the output membership function.

Table 4 The structural parameters of both buildings in numerical example.

Floor (i)	Building A			Building B		
	m_i (t)	$k_i \times 10^6$ (kN/m)	$c_i \times 10^3$ (kN sec/m)	m_i (t)	$k_i \times 10^4$ (kN/m)	$c_i \times 10^3$ (kN sec/m)
1	800	1.4	1.190	215	4.679	0.604
2	800	1.4	1.190	201	4.76	0.644
3	800	1.4	1.190	201	4.68	0.684
4	800	1.4	1.190	200	4.5	0.724
5	800	1.4	1.190	201	4.5	0.752
6	800	1.4	1.190	201	4.5	0.806
7	800	1.4	1.190	201	4.5	0.604
8	800	1.4	1.190	203	4.37	0.644
9	800	1.4	1.190	203	4.37	0.684
10	800	1.4	1.190	203	4.37	0.724
11	800	1.4	1.190			
12	800	1.4	1.190			
13	800	1.4	1.190			
14	800	1.4	1.190			
15	800	1.4	1.190			
16	800	1.4	1.190			
17	800	1.4	1.190			
18	800	1.4	1.190			
19	800	1.4	1.190			
20	800	1.4	1.190			

Table 5 The natural frequencies of model examples used for MR dampers.

Frequency (Hz)	Building A	Building B
ω_1	0.510	1.148
ω_2	1.527	3.371
ω_3	2.535	5.443
ω_4	3.529	7.347
ω_5	4.501	9.075
ω_6	5.447	
ω_7	6.361	
ω_8	8.072	
ω_9	8.860	

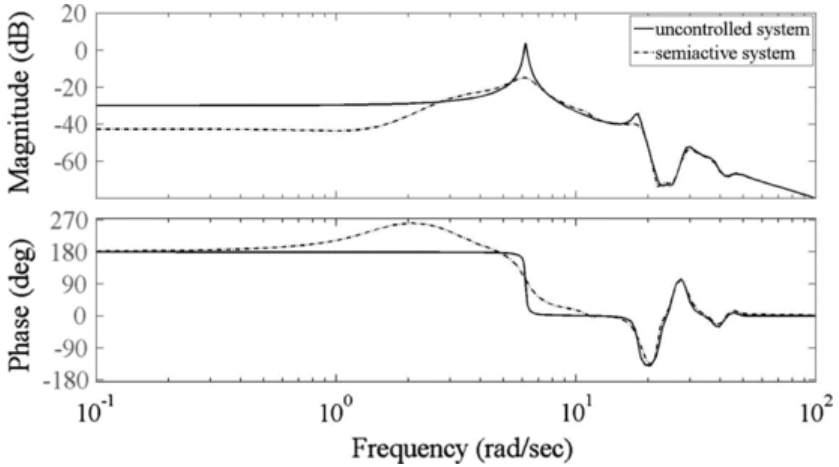

Fig. 4 Transfer function from external excitation to the top floor displacement of Building A.

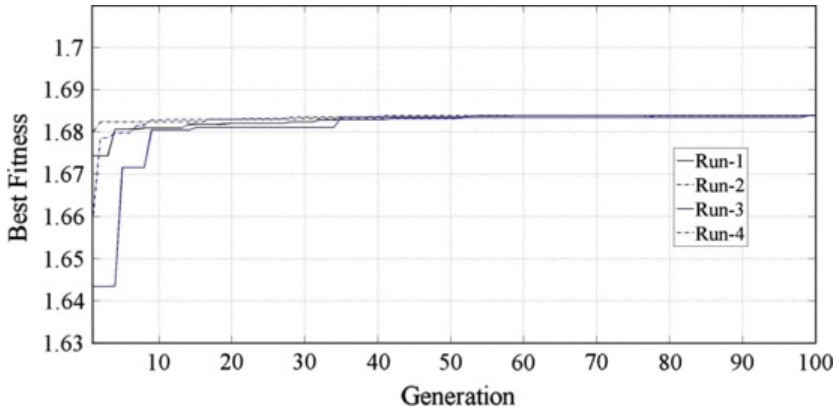

Fig. 5 Evolving best fitness with binary coded GA.

Before demonstrating the multiple objective functions into a single-objective function, the performance of MR dampers is investigated in reducing the seismic response of adjacent buildings. Firstly, five MR dampers installed at each of the ten floors in numerical example. All fifty dampers have the same input voltage. Nonlinear random vibration analyses using the 4th order Runge Kutta method is performed while varying the uniform input voltage from 0 to 10 V, which leads to the variation of the damping capacity of the MR dampers. Hysteresis behavior of MR damper under four control strategies, namely, passive-off, passive-on, semiactive-LQR and semiactive-for earthquakes is shown in Fig. 6. Fig. 7 shows the maximum values of inter-storey drifts for the variety of the uniform input voltage of the MR dampers. For decreasing the maximum inter-storey drift of the adjacent system, it is explained that an optimal value for the uniform input voltage of the MR dampers exists in a coupled structure system. In this numerical example, the optimal input voltage of the MR dampers is 5.6 V for the uniform distribution of the 50-MR damper system in Kobe 1995 earthquake, while the optimal input voltage is 3.1 V in El-Centro 1940 earthquake.

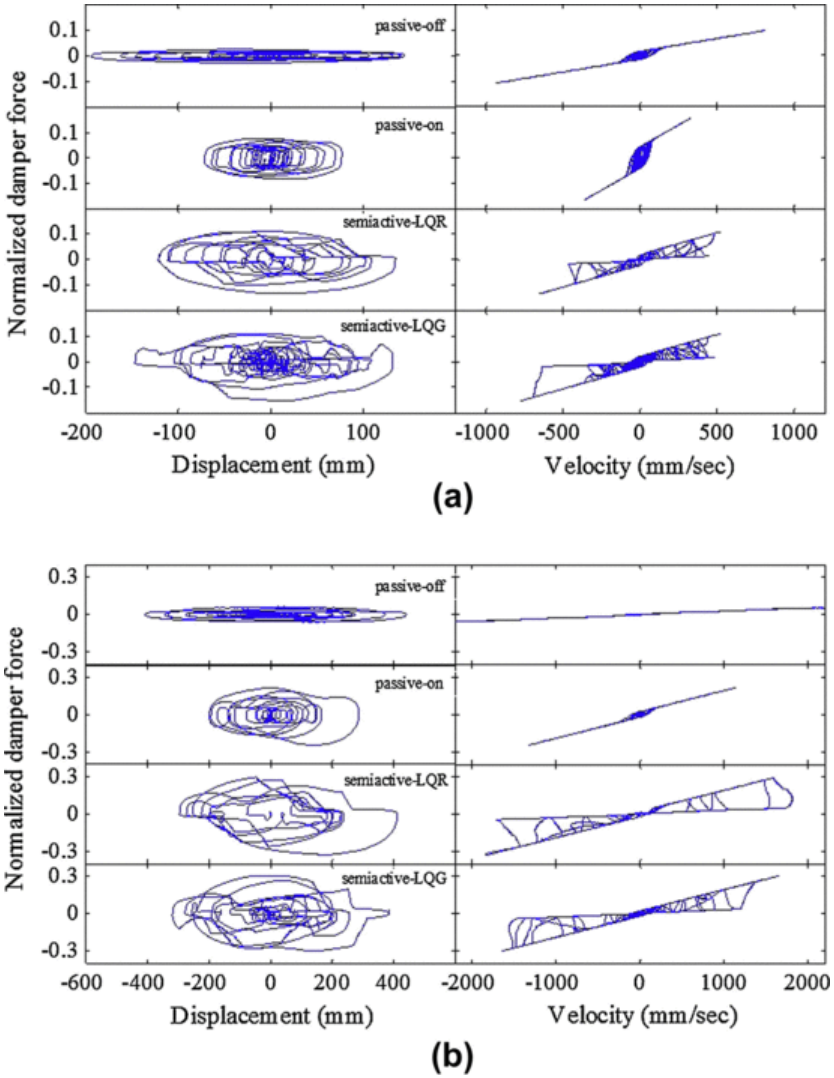

Fig. 6 The behavior of MR damper under (a) 1940 El-Centro earthquake and (b) 1995 Kobe earthquake.

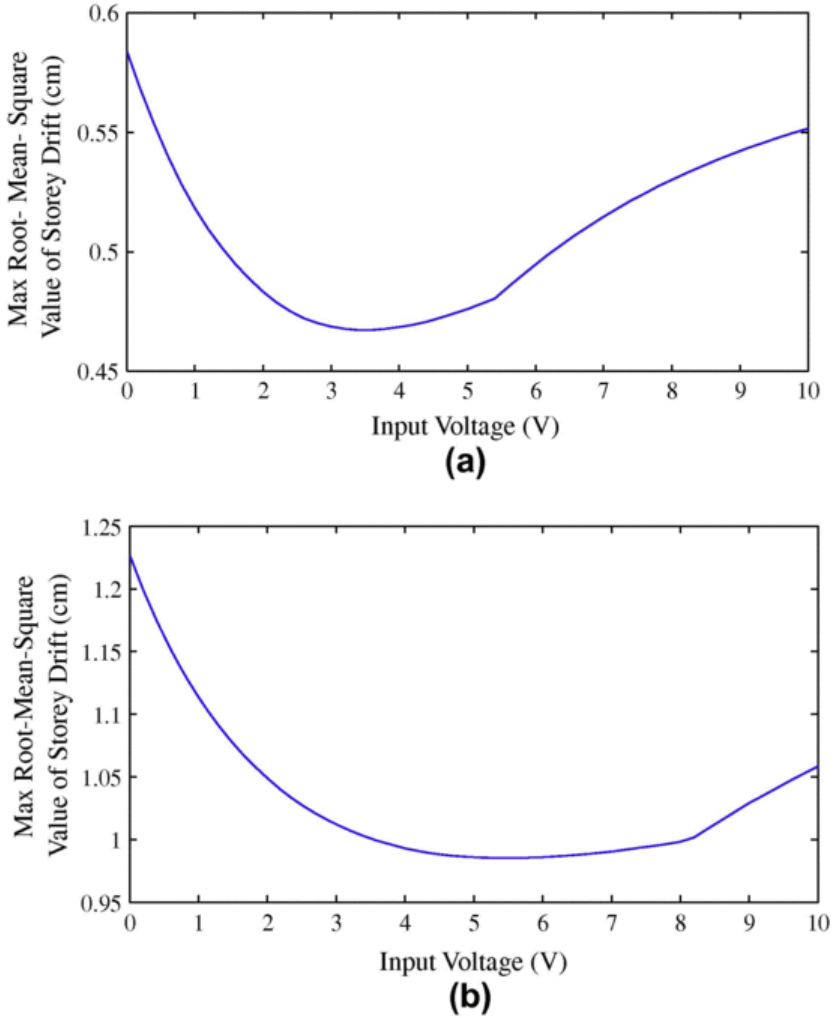

Fig. 7 Control performance of MR dampers with uniform input voltages under (a) the 1940 El-Centro earthquake and (b) the 1995 Kobe earthquake scaled to 0.8 g.

Using the MR damper is important in damping capacity that can be easily adjusted by modulating the input voltage, without costly replacements or adjustments. In other words, varying the input voltages of the dampers is feasible in order to achieve an optimal performance. Hence, the results of the peak top floor displacement, acceleration and normalized base shear of the adjacent buildings using the optimum uniform voltage (OUV) is evaluated with the other control strategies used in this study. It is noted that varying the uniform input voltage *vdi* from 0 to 2.25 V for each storey is also conducted by means of the rule-based in fuzzy logic control in GA. Table 6 shows the fuzzy rules generated by GA. The optimal input voltages for each floor level are examined by an SOGA optimization for the given example of five MR dampers installed at each of the ten floors. The results of GA optimization are shown and a fuzzy logic controller is identified for both the multi-input single-output (MISO). This rule base obtained by GA establishes the correlation between the selected displacement inputs and the command voltage sent to MR damper when (kN m). K_θ and 10^9 represent the top floor displacements of the Building A and Building B, respectively. When (kN m) in Eq. (14), the multi-objective problem degenerates into a single-objective problem. The proposed strategy has the capability to mitigate the displacement response significantly while keeping the storey drift response at a low level. For GA, the population size is taken as 12 members and the upper limit on the number of generations is taken as 100. Based on an elitist model, in order to perform evolutionary operations, proportional selection and one-point crossover are chosen in FLC combined to GA.

Table 6 Fuzzy rule-base generated by GA in Case I under (a) El-Centro 1940 ground motion (b) Kobe 1995 ground motion scaled to 0.8 g.

x_{20}	x_{30}				
	NL	NS	ZO	PS	PL
(a) El-Centro 1940 ground motion					
NL	L	L	L	L	M
NS	ZO	M	L	L	S
ZO	S	ZO	S	M	M
PS	M	S	L	M	M
PL	M	M	L	S	L
(b) Kobe 1995 ground motion scaled to 0.8 g					
NL	ZO	L	S	S	S
NS	M	S	L	L	L
ZO	S	S	S	ZO	M
PS	ZO	M	ZO	S	ZO
PL	S	ZO	S	S	M

Results of the damper locations in Case I obtained by Hadi and Uz [56] are compared with the fuzzy controller combined by GA (GAF). In Table 7, using the optimum uniform voltage (OUV) and fuzzy controller combined by GA (GAF), the significant reduction for both buildings is observed under El-Centro 1940 earthquake although these proposed methods are not effectives in both buildings under Kobe 1995 earthquake. In Table 8, the top floor drift inter-storey responses show that the percentage reductions for Building A under GAF strategy as compared to the uncontrolled case are: 8.0 and 9.0, while the corresponding response reductions for Building B are 19.5 and 33.1 for El-Centro 1940 and Kobe 1995 earthquakes, respectively. However, a marginal increase in response is seen under semi-active controllers (9 V) for Building B under El-Centro 1940 earthquake. The proposed GAF control strategy and the uncontrolled case show that the correlation established by GA is effective. For Building B, a significant reduction of the normalized base shear responses is shown in the last column in Table 9. As expected, Table 10 shows an increase in damper voltage has shown increase in force of the MR dampers. Using the proposed GAF controller, the damper force of all MR dampers at the top floor level of Building B is kept at a low level compared to the other strategies in Table 10 under both the considered earthquakes. In Case II, only alternate floors of the lower building connected with the adjoining floors of the higher building are considered for MR dampers. The number of MR dampers *ndii* at each storey levels is minimized by using GA for economical benefits. At the same time, the input voltages are determined based on the optimal number of MR dampers for each storey.

Table 7 Peak top floor displacement under different control strategies for Case I.

Earthquakes	Buildings	UNC	Case I										
			Off	Passive-on			LQR–CVL			H_2/LQG–CVL			OUV	GAF
				3 V	6 V	9 V	3 V	6 V	9 V	3 V	6 V	9 V		
El Centro, 1940	A	26.6	22.9	20.1	19.0	19.8	21.8	21.2	20.7	21.6	20.9	20.4	20.2	21.9
	B	17.1	8.1	8.6	10.4	11.5	8.4	8.6	8.7	8.6	9.1	9.6	8.8	7.9
Kobe, 1995	A	61.3	59.4	57.4	58.0	59.2	56.0	55.2	54.8	57.4	56.7	56.3	58.0	58.8
	B	48.0	35.0	25.6	30.6	32.9	29.6	27.5	26.0	30.5	27.7	25.5	30.7	29.1

Note: the displacement indicated is in ×10 mm. UNC: Uncontrolled.

Table 8 Peak top floor drift inter-storey under different control strategies for Case I.

Earthquakes	Buildings	UNC	Case I										
			Off	Passive-on			LQR–CVL			H_2/LQG–CVL			OUV	GAF
				3 V	6 V	9 V	3 V	6 V	9 V	3 V	6 V	9 V		

El Centro, 1940	A	0.25	0.24	0.23	0.23	0.23	0.23	0.22	0.22	0.22	0.22	0.22	0.23	0.23
	B	0.41	0.26	0.23	0.28	0.31	0.29	0.37	0.43	0.33	0.41	0.51	0.32	0.33
Kobe, 1995	A	0.88	0.83	0.81	0.84	0.87	0.75	0.74	0.75	0.81	0.82	0.83	0.84	0.80
	B	1.54	1.19	1.11	0.98	1.07	0.84	0.99	1.21	0.84	0.88	1.02	1.35	1.03

Table 9 Peak normalized base shear under different control strategies for Case I.

Earthquakes	Buildings	UNC	Case I										
			Off	Passive-on			LQR–CVL			H_2/LQG–CVL			OUV	GAF
				3 V	6 V	9 V	3 V	6 V	9 V	3 V	6 V	9 V		
El Centro, 1940	A	0.20	0.19	0.17	0.16	0.16	0.18	0.17	0.17	0.17	0.16	0.16	0.17	0.18
	B	0.57	0.28	0.35	0.40	0.40	0.29	0.30	0.31	0.29	0.32	035	0.35	0.28
Kobe, 1995	A	0.40	0.40	0.41	0.42	0.43	0.39	0.39	0.38	0.38	0.37	0.37	0.42	0.41
	B	1.56	1.10	0.71	0.90	1.00	0.88	0.80	0.76	0.94	0.83	0.74	0.88	0.89

Table 10 Peak damper force of all MR dampers at the top floor level of the lower building under different control strategies for Case I.

Earthquakes	Case I											
	Off	Passive-on			LQR–CVL			H_2/LQG–CVL			OUV	GAF
		3 V	6 V	9 V	3 V	6 V	9 V	3 V	6 V	9 V		
El-Centro, 1940	54	127	166	203	181	287	379	192	315	426	127	80
Kobe, 1995	126	346	499	590	420	692	955	402	637	864	476	254

Note: The damper force indicated in kN.

The optimal input voltages for each floor level by SOGA and NSGA II optimizations are determined for Case II in the given example in this study. The number of MR dampers and the corresponding command voltages are chosen as the design variables. Fig. 8 shows the variable distribution of the command voltages corresponding to the optimal uniform distribution under the considered earthquakes. The multi objective optimization is conducted by NSGA II to obtain the Pareto-optimal solutions as shown in Fig. 8. In order to provide the optimal damper systems in terms of cost-saving, another objective function is selected as the number of MR dampers to be minimized. Hence, the max root mean square (r.m.s.) storey drift of the coupled buildings and the total number of the MR dampers are the two objective functions, which are the vertical and horizontal axes in Fig. 8, respectively. It is noteworthy that the total number of the MR dampers is explicitly reduced by means of improved control performance using GA and NSGA II optimizations. In other words, the performance efficiency of the damper system and the cost effectiveness are considered in terms of the vertical and horizontal axes. This study achieves a similar level of seismic performance even with significantly reduced number of dampers with the help of the proposed strategies. At the same time, input damper voltage is optimally determined. The maximum inter-storey drifts by the uniform and varying voltages are 4.67 mm and 4.62 mm as shown Figs. 7 and 8.

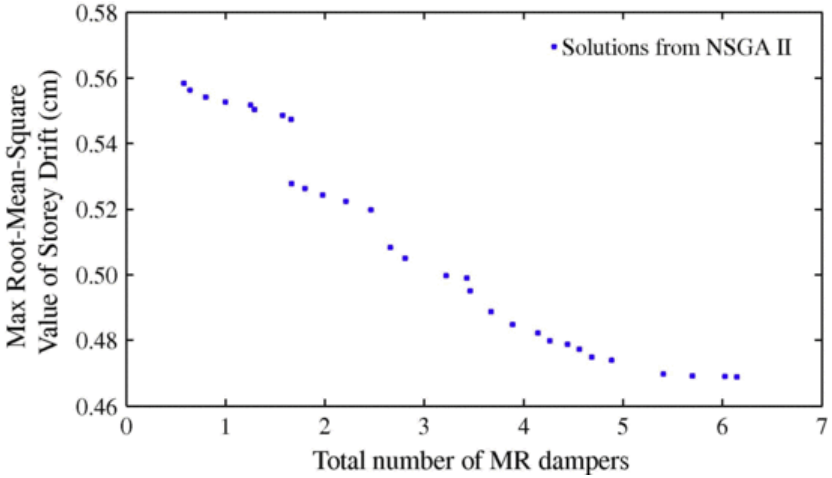

Fig. 8 The variation values of design variables under the 1940 El-Centro Earthquake using NSGA II optimization.

The optimum uniform voltage (OUV) is 3.1 V for El-Centro 1940 earthquake while for Kobe 1995 the OUV is 5.6 V under the uniform distribution of the 50 MR damper systems. The total number of MR dampers are reduced from 50 to 6 for El-Centro 1940 and 8 for Kobe 1995 earthquake as referred to Fig. 9. The number of MR dampers (*ndii*) and the variable distribution of the input voltage (*vdi*) are designed by a simple GA. The total control voltage required to operate the MR dampers in the uniform distribution system turns out to be 155.0 V for El-Centro 1940 and 280.0 V for Kobe 1995 earthquake, whereas the variable distribution system uses a total of 52.1 V for El-Centro 1940 and 66.4 V for Kobe 1995 ground motion as shown in Fig. 9(d–g). The optimal system determined by the NSGA in this section is also denoted, which uses 6 or 8 MR dampers with optimal input voltage at each floor according the related earthquakes. The response parameters of interest for adjacent buildings are the peak top floor x_i, the peak floor drift d_i, the peak normalized base shear F_o and damper force F_{mr} as given through Tables 11 and 14.

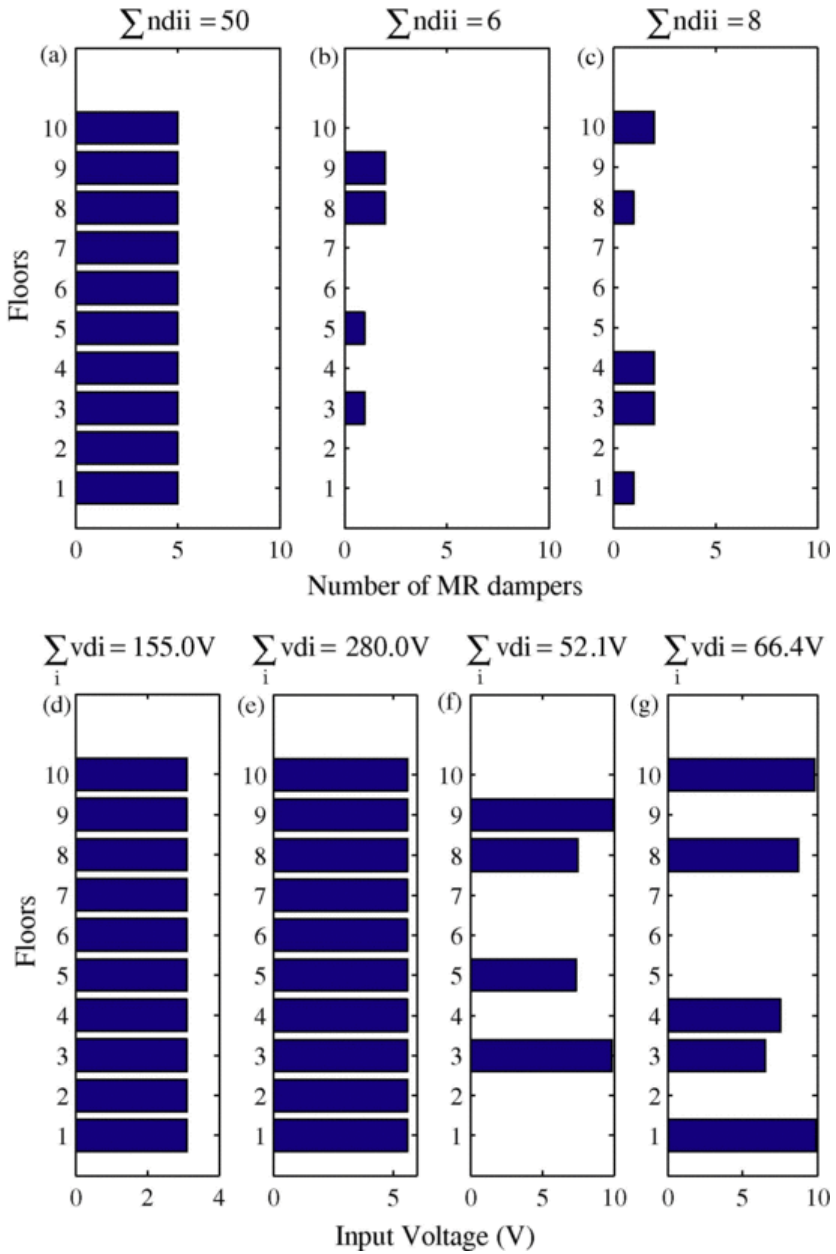

Fig. 9 Installation MR dampers (a) uniform distribution, (b) variation distribution in El-Centro 1940, (c) in Kobe 1995 earthquakes, uniform distribution of (d) El-Centro 1940, (e) Kobe 1995, variation distribution of (f) El-Centro 1940 and (g) Kobe 1995 for input voltage of MR dampers.

Table 11 Peak top floor displacement under different control strategies for Case II.

Earthquakes	Buildings	UNC	Case II				
			Off	Passive-on	LQR–CVL	H_2/LQG–CVL	GA

				3 V	6 V	9 V	3 V	6 V	9 V	3 V	6 V	9 V	
El Centro, 1940	A	26.6	25.8	23.7	22.8	22.3	24.1	22.9	22.7	24.3	23.5	23.3	22.4
	B	17.1	13.8	9.4	8.06	7.75	10.9	10.3	10.2	11.9	11.0	10.4	7.79
Kobe, 1995	A	61.3	61.0	60.1	59.3	58.8	59.8	58.8	58.1	60.5	60.2	60.0	58.9
	B	48.0	45.9	39.8	35.2	31.4	42.1	40.1	38.7	42.7	40.1	38.0	31.5

Although the difference in the maximum inter-storey drift is not significant, the optimally designed variable distribution system use less damping capacity with improved control performance in GA and NSGA II optimizations. Table 11 shows the peak top floor displacement of the coupled systems under damper location Case II in terms of control strategies. It is observed that numerical results given by the last column in Table 11, whose control strategy name is GA, shows the effectiveness of the newly generated number of MR dampers and command voltage values. The percentage reduction of the drift inter-storey for Building B under passive-on strategy for Case II (6 V) in Table 12 as compared to the uncontrolled are 14.6 and 5.7 under El-Centro 1940 and Kobe 1995 earthquakes, respectively, and the corresponding reductions under semiactive controller based LQR are 2.44 and 7.1. Similar trends are also observed under damper location Case II and command voltage 3 V and 9 V. This shows that the percentage reduction under passive-on is better in comparison to semiactive strategy. Table 13 shows the overall base shear reduction with the optimum command voltage obtained by GA and NSGA II optimizations. In Table 14, it is noteworthy that the peak damper force of all MR dampers increased compared to Case I although the total number of the MR dampers decreased. However, increase in the damper forces of Case II is observed because of increase in command voltage under all control strategies. This shows that connecting only at the alternative floors reduces the cost of dampers significantly by eighty percent and response reduction is also explicitly observed. The increase in voltage causes to increase in damper stiffness, therefore, attracts more force according to formulations as shown in Eqs. (3) and (4).

Table 12 Peak top floor drift inter-storey under different control strategies for Case II.

Earthquakes	Buildings	UNC	Case II										
			Off	Passive-on			LQR–CVL			H_2/LQG–CVL			GA
				3 V	6 V	9 V	3 V	6 V	9 V	3 V	6 V	9 V	
El Centro, 1940	A	0.25	0.25	0.25	0.24	0.23	0.24	0.24	0.24	0.25	0.24	0.23	0.23
	B	0.41	0.46	0.37	0.35	0.34	0.40	0.40	0.41	0.40	0.39	0.43	0.34
Kobe, 1995	A	0.88	0.87	0.85	0.83	0.82	0.84	0.82	0.81	0.87	0.87	0.86	0.83
	B	1.54	1.49	1.40	1.34	1.30	1.41	1.43	1.48	1.44	1.41	1.39	1.32

Table 13 Peak normalized base shear under different control strategies for Case II.

Earthquakes	Buildings	UNC	Case II										
			Off	Passive-on			LQR–CVL			H_2/LQG–CVL			GA
				3 V	6 V	9 V	3 V	6 V	9 V	3 V	6 V	9 V	
El Centro, 1940	A	0.20	0.19	0.19	0.19	0.18	0.18	0.18	0.18	0.18	0.19	0.19	0.18
	B	0.57	0.47	0.32	0.28	0.26	0.37	0.34	0.33	0.41	0.38	0.36	0.27
Kobe, 1995	A	0.40	0.39	0.40	0.40	0.40	0.39	0.39	0.39	0.40	0.39	0.39	0.40
	B	1.56	1.47	1.26	1.10	0.97	1.33	1.24	1.19	1.35	1.25	1.16	0.98

Table 14 Peak damper force of all MR dampers at the top floor level of the lower building under different control strategies for Case II.

Response	Case II				
	Off	Passive-on	LQR–CVL	H_2/LQG–CVL	GA

			3 V	6 V	9 V	3 V	6 V	9 V	3 V	6 V	9 V	
F_{mr}	E	82	240	360	464	249	397	537	270	430	478	489
	K	176	578	858	1085	610	978	1341	624	997	1329	1177

Note: H_2 is the damper force indicated in kN, E: represents the 1940 El-Centro, K: represents the 1995 Kobe earthquake scaled to 0.8 g.

6 Conclusions

For enhancing the seismic performance of two adjacent buildings, an optimal design method for nonlinear hysteretic dampers is proposed. The stochastic linearization method helps estimate the stochastic responses of adjacent buildings coupled by nonlinear dampers in an efficient manner. As a result, the optimal design process can avoid numerous nonlinear time-history analyses. The numerical example of 10- and 20-storey buildings coupled by MR dampers demonstrate that the proposed optimal design approach can systematically achieve enhanced seismic performance with economical efficiency. The proposed GAF and GA methods for the output voltage of MR dampers achieve enhanced seismic performance with economical efficiency. GAF shows better control in displacement and damper force response of Building A although all used strategies is better for the shorter building (Building B).

Appendix A

Notations

A	= system matrix in state space equation
A_c	= hysteresis loop parameters
a	= constant value
a_j	= each random number ($j = 1, 2, \ldots$ popsize) between 0 and 1
a_{a0}, a_{b0}	= proportional coefficients of Building A and Building B, respectively
B	= system matrix in state space equation
b_{a0}, b_{b0}	= proportional coefficients of Building A and Building B, respectively
C	= damping matrix
C_p	= constant value (1 or 2)
C_w	= regulation matrix
C_1	= damping matrix of Building A
C_2	= damping matrix of Building B
c_d	= damping of the damper
c_0	= hysteresis loop parameters of MR damper
c_{0a}	= hysteresis loop parameters of MR damper
c_{0b}	= hysteresis loop parameters of MR damper
c_1	= hysteresis loop parameters of MR damper
c_{1a}	= hysteresis loop parameters of MR damper
c_{1b}	= hysteresis loop parameters of MR damper
D	= zero matrix in Hamiltonian
D_w	= regulation matrix
d_i	= inter-storey drift of the ith floor in controlled system
d_{max}	= the peak uncontrolled floor drift
E	= system matrix in state space equation
E_1	= vector representing the influence of the related earthquake to Building A

E_2	= vector representing the influence of the related earthquake to Building B
F	= fitness function
f_d	= desired force matrix at the damper
f_{di}	= desired force at the ith damper
f_{mr}	= force matrix at the damper
$\|\widehat{G}_{\infty}$	= transfer function
$\|\widehat{G}_{\infty}\|$	= H_∞ norm of $\widehat{G}_{\infty}$
G^p	= individual in the population
g_{rj}^{pi}	= one variable in G^p
H_2	= control algorithm
H_∞	= control algorithm
$\boldsymbol{H}$	= Hamiltonian
H{}	= Heaviside function in Matlab
h_j	= bit string no. $(j+1)$ starting from right
i_s	= index
I	= identity vector
I, $\boldsymbol{I}$	= $(n+m)$ *and* $(2n+2m)$ identity matrices, respectively
J	= objective function
J	= performance index
J_1	= objective function to be minimized the displacement responses
J_2	= objective function to be minimized the inter-storey drift responses
j_s	= index
K	= stiffness matrix of all system
K	= gain matrix
K_1	= stiffness matrix of Building A
K_2	= stiffness matrix of Building B
k_d	= stiffness of the damper
k_0	= hysteresis loop parameters of MR damper
k_1	= hysteresis loop parameters of MR damper
L_i	= lower bound value of design variable
l_m	= length of sub-chromosome
M	= total mass matrix
M_1	= mass matrix of Building A
M_2	= mass matrix of Building B
m	= number of floors in Building B
m_i, m_j	= mass $(i = 1, 2, \ldots, n)$ $(j = 1, 2, \ldots, m)$

m_a	= number of measurements
N_d	= total number of dampers at all floors
n	= number of floors in Building A
n_a	= number of actuators
nbits	= number of bits
n_d	= hysteresis loop parameters of MR damper
n_r	= random number
P	= Riccati matrix, matrix of Lyapunov equation
P_i	= significant digit
P_1	= control force location matrix of Building A
P_2	= control force location matrix of Building B
p_c	= crossover rate
p_m	= mutation rate
Q	= state weighting matrix
q_j	= probability of crossover
R	=unit matrix having a random coefficient
R	= scalar control force weighting matrix
R	= control force weighting matrix
r_i	= real number of a design variable
S	= solution of the algebraic Ricatti equation
$S_{\ddot{x}_g\ddot{x}_g}, S_{v_i v_i}$	= spectral density function of acceleration and measurement noise
s	= difference between the number floors of both buildings
s	= Laplace variable
t	= time
t_i	= integer mapping of a binary string
U_i	= upper bound value of design variable
$u, \dot{u}$	= control voltage and output of a first-order filter
V_{max}	= maximum voltage
v	= input voltages of the first order filter
v	= measurement noise vector
$X, \dot{X}, \ddot{X}$	= total displacement, velocity and acceleration matrices, respectively
X_1, X_2	= displacement matrix of Building A and Building B, respectively
$\dot{X}_1, \dot{X}_2$	= velocity matrix of Building A and Building B, respectively
$\ddot{X}_1, \ddot{X}_2$	= acceleration matrix of Building A and Building B, respectively
$\ddot{X}_g$	= acceleration vector of the related earthquake

x^{max}	= maximum displacement of the uncontrolled system
$x_i, \dot{x}_i$	= displacement and velocity of the ith floor level, respectively
x_0	= initial displacement of the damper
y_m	= vector of measured outputs
$y_i, \dot{y}_i$	= internal pseudo-displacement
$z_{di}, \dot{z}_{di}$	= evolutionary variable
α, α_a, α_b	= hysteresis loop parameters of MR damper
α_c	= weighting coefficient (1 or 2)
β	= hysteresis loop parameters of MR damper
γ, γ_u, γ_l	=a random number, upper bound and lower bound of a positive number
ω_{ai}, $\omega_{aj}\omega_{bi}$, ω_{bj}	= structural modal frequencies of modes i and j of both buildings
ξ_{ai}, $\xi_{aj}\xi_{bi}$, ξ_{bj}	= structural damping ratios for modes i and j of both buildings
μ	=constant to scale the fitness function
η	= time constant of the first-order filter
Λ	= system matrix in state space equation
Γ	= vector representing the influence of the related earthquake to all system
0	= zero matrix

References

[1]

W.S. Zhang and Y.L. Xu, Dynamic characteristics and seismic response of adjacent buildings linked by discrete dampers, *Earthq Eng Struct Dynam* **28** (10), 1999, 1163–1185.

[2]

H.P. Zhu, D.D. Ge and X. Huang, Optimum connecting dampers to reduce the seismic responses of parallel structures, *J Sound Vib* **330** (9), 2011, 1931–1949.

[3]

Z. Yang, Y.L. Xu and X.L. Lu, Experimental seismic study of adjacent buildings with fluid dampers, *J Struct Eng* **129** (2), 2003, 197–205.

[4]

W.S. Zhang and Y.L. Xu, Vibration analysis of two buildings linked by Maxwell model-defined fluid dampers, *J Sound Vib* **233** (5), 2000, 775–796.

[5]

S.-H. Lee, J.-H. Park, S.-K. Lee and K.-W. Min, Allocation and slip load of friction dampers for a seismically excited building structure based on storey shear force distribution, *Eng Struct* **30** (4), 2008, 930–940.

[6]

A.V. Bhaskararao and R.S. Jangid, Seismic analysis of structures connected with friction dampers, *Eng Struct* **28** (5), 2006, 690–703.

[7]

C.-L. Ng and Y.-L. Xu, Seismic response control of a building complex utilizing passive friction damper: experimental investigation, *Earthq Eng Struct Dynam* **35** (6), 2006, 657–677.

[8]

A.V. Bhaskararao and R.S. Jangid, Seismic response of adjacent buildings connected with friction dampers, *Bull Earthq Eng* **4** (1), 2006, 43–64.

[9]

Hadi MNS, Uz ME. Investigating the optimal passive and active vibration controls of adjacent buildings based on performance indices using genetic algorithms. J Eng Optim; 2013 [in press].

[10]

Y.L. Xu and W.S. Zhang, Closed-form solution for seismic response of adjacent buildings with linear quadratic Gaussian controllers, *Earthq Eng Struct Dynam* **31** (2), 2002, 235–259.

[11]

Z.G. Ying, Y.Q. Ni and J.M. Ko, Stochastic optimal coupling-control of adjacent building structures, *Comput Struct* **81** (30–31), 2003, 2775–2787.

[12]

M.-G. Yang, C.-Y. Li and Z.-Q. Chen, A new simple non-linear hysteretic model for MR damper and verification of seismic response reduction experiment, *Eng Struct* **52**, 2013, 434–445.

[13]

J.N. Yang and A.K. Agrawal, Semi-active hybrid control systems for nonlinear buildings against near-field earthquakes, *Eng Struct* **24** (3), 2002, 271–280.

[14]

S.-Y. Ok, J. Song and K.-S. Park, Optimal design of hysteretic dampers connecting adjacent structures using multi-objective genetic algorithm and stochastic linearization method, *Eng Struct* **30** (5), 2008, 1240–1249.

[15]

S.D. Bharti, S.M. Dumne and M.K. Shrimali, Seismic response analysis of adjacent buildings connected with MR dampers, *Eng Struct* **32** (8), 2010, 2122–2133.

[16]

G. Yan and L.L. Zhou, Integrated fuzzy logic and genetic algorithms for multi-objective control of structures using MR dampers, *J Sound Vib* **296** (1–2), 2006, 368–382.

[17]

O. Yoshida and S.J. Dyke, Seismic control of a nonlinear benchmark building using smart dampers, *J Eng Mech* **130** (4), 2004, 386–392.

[18]

J. Kim, J. Ryu and L. Chung, Seismic performance of structures connected by viscoelastic dampers, *Eng Struct* **28** (2), 2006, 183–195.

[19]

S.J. Dyke, , B.F. Spencer, Jr, M.K. Sain, and J.D. Carlson, , Modeling and control of magnetorheological dampers for seismic response reduction, *Smart Mater Struct* **5** (5), 1996, 565.

[20]

S.J. Dyke, , J.B.F. Spencer, , P. Quast, , M.K. Sain, , D.C. Kaspari, Jr and T.T. Soong, , Acceleration feedback control of MDOF structures, *J Eng Mech* **122** (9), 1996, 907–918.

[21]

Y.Q. Ni, J.M. Ko and Z.G. Ying, Random seismic response analysis of adjacent buildings coupled with non-linear hysteretic dampers, *J Sound Vib* **246** (3), 2001, 403–417.

[22]

K.-S. Park and S.-Y. Ok, Optimal design of actively controlled adjacent structures for balancing the mutually conflicting objectives in design preference aspects, *Eng Struct* **45**, 2012, 213–222.

[23]

H.-S. Kim and J.-W. Kang, Semi-active fuzzy control of a wind-excited tall building using multi-objective genetic algorithm, *Eng Struct* **41**, 2012, 242–257.

[24]

G. Yang, , B.F. Spencer, Jr, J.D. Carlson, and M.K. Sain, , Large-scale MR fluid dampers: modeling and dynamic performance considerations, *Eng Struct* **24** (3), 2002, 309–323.

[25]

J.E. Luco and F.C.P. De Barros, Optimal damping between two adjacent elastic structures, *Earthq Eng Struct Dynam* **27** (7), 1998, 649–659.

[26]

K. Bigdeli, W. Hare and S. Tesfamariam, Configuration optimization of dampers for adjacent buildings under seismic excitations, *Eng Optim* 2012, 1–19.

[27]

Uz ME. University of Wollongong. School of Civil M., Environmental E., Improving the dynamic behaviour of adjacent buildings by connecting them with fluid viscous dampers; 2009.

[28]

Uz ME, Hadi MNS. Dynamic analyses of adjacent buildings connected by fluid viscous dampers. In: Seventh world conference on earthquake resistant engineering structures ERES VII. Limassol, Cyprus, Wessex Institute of, Technology, vol. 150; 2009. p. 139–50.

[29]

Uz ME. Optimum design of semi-active dampers between adjacent buildings of different sizes subjected to seismic loading including soil–structure interaction. Doctor of Philosophy, School of Civil, Mining and Environmental Eng, University of Wollongog; 2013.

[30]

C.C. Patel and R.S. Jangid, Seismic response of dynamically similar adjacent structures connected with viscous dampers, *IES J Part A: Civil Struct Eng* **3** (1), 2009, 1–13.

[31]

M.D. Symans and S.W. Kelly, Fuzzy logic control of bridge structures using intelligent semi-active seismic isolation systems, *Earthq Eng Struct Dynam* **28** (1), 1999, 37–60.

[32]

L. Zhou, C. Chang and L. Wang, Adaptive fuzzy control for nonlinear building-magnetorheological damper system, *J Struct Eng* **129** (7), 2003, 905–913.

[33]

Arfiadi Y. Optimal passive and active control mechanisms for seismically excited buildings. Doctor of Philosophy Thesis, Faculty of Engineering, University of Wollongong; 2000. <http://ro.uow.edu.au/theses/1836>.

[34]

Y.-J. Kim and J. Ghaboussi, Direct use of design criteria in genetic algorithm-based controller optimization, *Earthq Eng Struct Dynam* **30** (9), 2001, 1261–1278.

[35]

Y. Arfiadi and M.N.S. Hadi, Passive and active control of three-dimensional buildings, *Earthq Eng Struct Dynam* **29** (3), 2000, 377–396.

[36]

Y. Arfiadi and M.N.S. Hadi, Optimal direct (static) output feedback controller using real coded genetic algorithms, *Comput Struct* **79** (17), 2001, 1625–1634.

[37]

Y. Arfiadi and M.N.S. Hadi, Continuous bounded controllers for active control of structures, *Comput Struct* **84** (12), 2006, 798–807.

[38]

Y. Arfiadi and M.N.S. Hadi, Optimum placement and properties of tuned mass dampers using hybrid genetic algorithms, *Int J Optim Civil Eng* **1**, 2011, 167–187.

[39]

M.N.S. Hadi and Y. Arfiadi, Optimum design of absorber for MDOF structures, *J Struct Eng* **124** (11), 1998, 1272–1280.

[40]

Y. Wang and S. Dyke, Modal-based LQG for smart base isolation system design in seismic response control, *Struct Control Health Monit* **20** (5), 2013, 753–768.

[41]

P.Y. Lin, P.N. Roschke and C.H. Loh, Hybrid base-isolation with magnetorheological damper and fuzzy control, *Struct Control Health Monit* **14** (3), 2007, 384–405.

[42]

A.S. Ahlawat and A. Ramaswamy, Multiobjective obtimal absorber system for torsionally coupled seismically excited structures, *Eng Struct* **25**, 2003, 941–950.

[43]

S. Pourzeynali, H.H. Lavasani and A.H. Modarayi, Active control of high rise building structures using fuzzy logic and genetic algorithms, *Eng Struct* **29** (3), 2007, 346–357.

[44]

B.F. Spencer, Jr, S.J. Dyke, , M.K. Sain, and J.D. Carlson, , Phenomenological model for magnetorheological dampers, *J Eng Mech* **123** (3), 1997, 230–238.

[45]

Hadi MNS, Uz ME. Investigating the optimal passive and active vibration controls of adjacent buildings based on performance indices using genetic algorithms. J Eng Optim; 2013 [in press].

[46]

S.-Y. Ok, J. Song and K.-S. Park, Optimal performance design of bi-tuned mass damper systems using multi-objective optimization, *KSCE J Civil Eng* **12** (5), 2008, 313–322.

[47]

D.E. Goldberg, Genetic algorithms in search, optimization and machine learning, 1989, Addison-Wesley; Reading (MA).

[48]

N. Srinivas and K. Deb, Muiltiobjective optimization using nondominated sorting in genetic algorithms, *Evol Comput* **2** (3), 1994, 221–248.

[49]

J.H. Holland, Adaptation in natural and artificial systems, 1975, The University of Michigan Press; Ann Arbor.

[50]

Jansen LM, Dyke SJ. Investigation of nonlinear control strategies for the implementation of multiple magnetorheological dampers. In: Proceedings of the engineering mechanics conference. Baltimore, Maryland: ASCE; 1999.

[51]

L.M. Jansen and S.J. Dyke, Semi-active control strategies for MR dampers: comparative study, *J Eng Mech* **126** (8), 2000, 795–803.

[52]

Z. Michalewicz, Genetic algorithms + data structures = evolution programs, 1996, Springer; Berlin.

[53]

K. Deb, Multi-objective genetic algorithms: problem difficulties and construction of test problems, *Evol Comput* **7** (3), 1999, 205–230.

[54]

S.-Y. Ok, D.-S. Kim, K.-S. Park and H.-M. Koh, Semi-active fuzzy control of cable-stayed bridges using magneto-rheological dampers, *Eng Struct* **29** (5), 2007, 776–788.

[55]

H.E. Kalasar, A. Shayeghi and H. Shayeghi, Seismic control of tall building using a new optimum controller based on GA, *Int J Appl Sci Eng Technol* **5** (2), 2009, 85.

[56]

Uz ME, Hadi MNS. Investigation of the optimal semi-active control strategies of adjacent buildings connected with magnetorheological dampers. J Eng Optim; 2013 [submitted for publication].

Highlights

- We use MR damper linkages to reduce seismic response of buildings.
- We use ~~Fuzzy~~ fuzzy controller with GA to reduce drift storey responses.
- The response control is better for the shorter building.
- Decreasing the number of dampers increases the system efficiency.

Queries and Answers

Query: Please confirm that given name(s) and surname(s) have been identified correctly.

Answer: yes

Query: Please update Refs. [9,45,56].

Answer:

References [9] and [56] are updated as below. Could you please remove Reference [45] in text and references list? It was the same with Reference [9]. Sorry for the repeated reference.

[9] M.N.S. Hadi and M.E. Uz, Investigating the optimal passive and active vibration controls of adjacent buildings based on performance indices using genetic algorithms. Engineering Optimization, DOI:10.1080/0305215X.2014.887704, 2014, 1-22.

[56] M.E. Uz and M.N.S. Hadi, Investigation of the optimal semi-active control strategies of adjacent buildings connected with magnetorheological dampers. Engineering Optimization, 2014 [In Revision for publication].